A comparative study of base isolation devices in light rail transit structure featured with lead rubber bearing and friction pendulum system

Santi Nuraini[1*], *Asdam* Tambusay[1], and *Priyo* Suprobo[1]

[1]Department of Civil Engineering, Institut Teknologi Sepuluh Nopember, Indonesia

Abstract. Advanced nonlinear analysis in light rail transit (LRT) structures has been undertaken to examine the influence of seismic isolation devices for reducing seismic demand. The study employed the use of two types of commercially available bearings, namely lead rubber bearing (LRB) and friction pendulum system (FPS). Six LRT structures, designed to be built in Surabaya, were modelled using computer-aided software SAP2000, where each of the three structures consisted of three types of LRB and FPS placed onto the pier cap to support the horizontal upper-structural member. Nonlinear static pushover and dynamic time history analysis with seven improved ground motion data was performed to gain improved insights on the behavioural response of LRT structures, allowing one to fully understand the supremacy of seismic isolations for protecting the structure against seismic actions. It is shown that both devices manage to isolate seismic forces, resulting in alleviation of excessive base shear occurring at the column. In addition, it is noticeable that the overall responses of LRB and FPS shows marginal discrepancies, suggesting both devices are interchangeable to be used for LRT-like structures.

Keywords: light rail transit, lead rubber bearing, friction pendulum system, SAP2000, pushover analysis, time history analysis

1 Introduction

Base isolation systems haves been broadly known as one of the pioneering advancements in structural engineering with the aim at protecting structures against earthquakes, allowing to reduce seismic demand and thereby maintaining structural integrity under significant seismic events [1-5]. The fundamental concept of base isolation systems is that it would be conceivable to extend the natural period of a structure as a means of providing additional damping and energy dissipation, thus preventing the structure to undergo severe damage under a major earthquake [6]. Over the last decades, elastomeric bearing systems have been successfully introduced in infrastructure projects and consequently, they have been used to support bridge structures with a flexible mount [7]. Furthermore, the systems applied have also been initially brought forward for its use in buildings. Recently, over 100 dwellings in

* Corresponding author: santinuraini1992@gmail.com

Europe and Australia have been built with rubber bearings with the purpose to specifically isolate the structures from vertical vibrations caused by underground machines. It has also proven to provide good performance for more than 40 years after construction, particularly for the structures that used thicker bearings as additional flexibility and the period shift could be achieved [8].

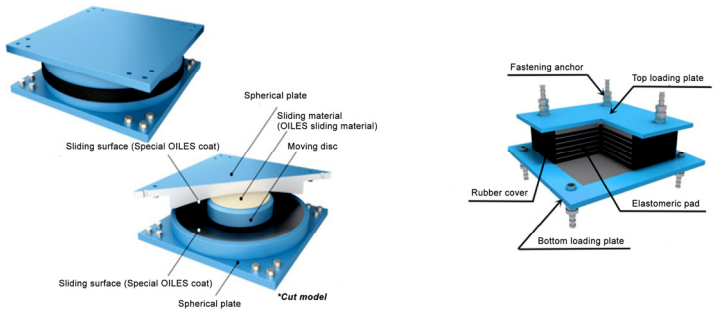

(a) (b)

Fig. 1. (a) Friction pendulum system and (b) lead rubber bearing [12]

To date, there are two types of sliding bearings which have been used in buildings and infrastructures. One type is flat sliding bearing that is used in combination with an elastomeric system, and another is pendulum bearing [9]. These bearings have unique properties and usability as they are made of different materials. In pendulum bearing, the triple friction pendulum (TFP) differs by a considerable extent to single friction pendulum system (FPS) where it is found in TFP that there are three friction pendulum mechanisms occurring in each bearing instead of just one. These mechanisms are being activated at different loading stages as the seismic demand gets stronger. On the other hand, the three mechanisms in FPS are achieved by using four concave surfaces, with sliding occurring on two of the surfaces at a given time [10]. In addition to the pendulum, lead rubber bearing (LRB) systems haves now been widely applied to construction projects across the globe. The system essentially works as an isolator which is designed using an elastomeric block, otherwise known as natural rubber or neoprene, reinforced with the metal bond. The device has one or more cylindrical lead cores [11]. The damping is resulted from the nature of the elastomeric mixture and lead cylinder, permitting to reduce acceleration and displacement through the distortion of the lead cylinder. Figure 1 presents the structural arrangements of the FPS and LRB devices.

Referring to the applicability of aforementioned bearing types, this current work provides an attempt to assess the seismic performance of LRT structures featured with two hybrid isolated devices (LRB and FPS). Nonlinear static pushover analysis is carried out to gain detailed insights with regard to the level of seismic performance of LRT structures under different types of the seismic isolation device. Additionally, further nonlinear dynamic time history analysis with artificially improved ground motions was undertaken to obtain the maximum lateral displacement. The feasibility of both seismic isolators is justified by analysis results.

2 Analytical model

As seen in Fig. 2, the typical model of reinforced concrete LRT structure comprised of four numbers of bored piles with diameter and depth of 1m and 30m respectively, a 2-metre-thick pile cap with cross-section of 5×5m, a bridge column with a height of 16 metres (pier) and rectangular cross-section of 2×2m, post-tensioned precast pier head, two custom-built

precast U-shape girder developed and patented by SYSTRA Consulting Group [13], and four bearings placed onto the pier head to support girders.

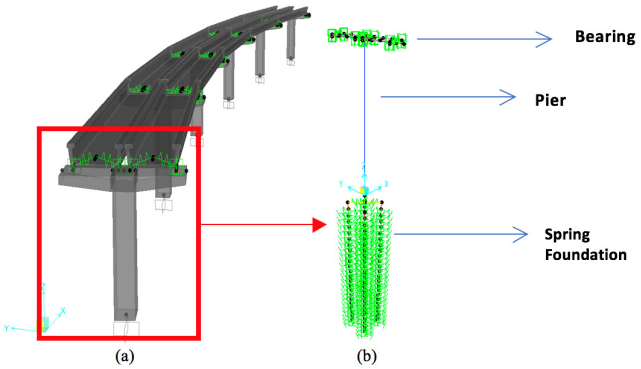

Fig. 2. Typical LRT structure modelled with SAP2000

Soil profiles were modelled by introducing horizontal and vertical constant point spring stiffness (kN/m) at each one-metre depth. The stiffness values were obtained using LPILE software and controlled manually using hand calculations. Design of seismic ground motion is determined based on the Indonesia earthquake provision SNI 1726:2012 [14] (drafted largely based on ASCE/SEI 7-10 [15].

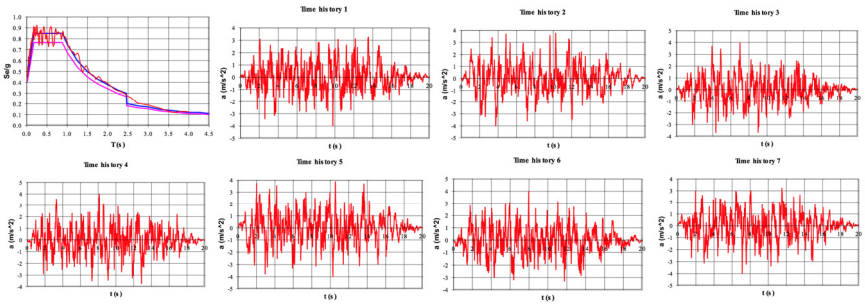

Fig. 3. Seven data of artificially-scale time history ground motion

The earthquake characteristics had peak ground acceleration (*PGA*) of 0.325*g*, mapped MCER, 5% damped, spectral response acceleration parameters at 0.2 (S_S) and 1 (S_1) second period, 0.50*g* and 0.25*g* respectively [16]. This data was put into SAP2000 to create a response spectrum chart which was based on the relationship of time (*t*) against pseudo acceleration (*g*). In addition, the data was also used to generate seven artificial time histories using scaling ground motion time history techniques as provided in the open source SMQKE software (see Fig. 3) [17].

Four seismic isolators were modelled using 2-joint link element with the length similar to the thickness of actual devices. Link/support types used in the analysis were 'lead rubber bearing' and 'triple pendulum isolator' for LRB and FPS respectively. It should be noted that directional properties of this model play an important role in altering the structural response. In this work, vertical movement (*U1*) was restrained, while for other horizontal translations (*U2* and *U3*), effective stiffness, stiffness, and yield strength were included in the simulation. However, it should be noted that the parameters were taken directly from the brochures (for clarity see Section 3 and 4). Prior iterative calculations were done using equations based on AASHTO LRFD [18] and NCHRP 20-7/Task 262(M2) [19]. These formulations are discussed in the next two sections.

Pushover analysis was performed using nonlinear static displacement control. Only the self-weight of the structure was considered in this simulation. The column tip was pushed up to one metre to foresee the nonlinear plateau of the structure and thereby allowing one to obtain the level of performance during plastic hinge mechanisms. Hinge property of the column and bored pile foundations were defined solely according to inherent moment-curvature of the column taking into consideration the interacting P-M2-M3.

The nonlinear dynamic analysis was performed using 'modal' time history type where the acceleration in the *x* and *y*-direction were defined using seven improved time history functions with a scale factor of one. The number of output time steps and output time step size were set properly so that the increments were found relatively small thereby giving smooth output in terms of hysteretic loops.

Table 1. LRB Material Properties [20].

Properties	LRB Type 1	LRB Type 2	LRB Type 3
Allowable bearing displacement	315 mm	315 mm	315 mm
Stiffness	4,3 kN/mm	5,53 kN/mm	3,15 kN/mm
Yield strength	80 kN	80 kN	80 kN
Height	252 mm	298 mm	356 mm

2.1 Lead rubber bearing

The properties of three different LRBs referred to in this study is shown in Table 1. Allowable bearing displacement was used herein as control of resulted displacement in the model. Stiffness and yield strength were used as nonlinear shear parameters. Formulations using iterative approach for obtaining the effective stiffness of bearing is expressed in Eq. (1) to Eq. (8), where Eq. (8) was also re-used to create isolated response spectrum function as specified in [19]. For the significances of each variable present in the equations see the Notation section.

$Q_{d,j} = n \times Q_{di}$	(1)	$d_{sub,j} = d - d_{isol,j}$	(8)
$K_{d,j} = n.K_{di}$	(2)	$F_{sub,j} = K_{sub,j}.d_{sub,j}$	(9)
$K_{sub,j} = \frac{1}{k}$	(3)	$T_{eff} = 2\pi\sqrt{\frac{K_{eff,j}}{g.\sum K_{eff}}}$	(10)
$\alpha_j = \frac{(K_{d,j}.d) + Q_{d,j}}{K_{\mathrm{sub},j}.d - Q_{d,j}}$	(4)	$\xi = \frac{2(Q_{dj}.d_{isol,j})}{\pi.K_{eff,\mathrm{j}}(d_{isol,j} + d_{sub,j})^2}$	(11)
$K_{eff,j} = \frac{\alpha_j.K_{sub,j}}{(1+\alpha_j)}$	(5)	$BL = \left(\frac{\xi}{0.05}\right)^{0.3}$	(12)
$d_{\mathrm{isol},j} = \frac{d}{(1+\alpha_j)}$	(6)	$d' = \left(\frac{g}{4\pi^2}\right)\left(\frac{S_{D1}.T_{eff}}{BL}\right)$	(13)
$K_{\mathrm{isol},j} = \frac{Q_{d,j}}{d_{\mathrm{isol},j}} + K_{\mathrm{d},j}$	(7)		

Iteration was stopped when the ratio of 'assumed' displacement over iterated displacement equals to unity. The final effective stiffness was then inputted to link properties in SAP2000.

2.2 Friction pendulum system

The material and section properties of three types of friction pendulum system are summarised in Table 2. Preliminary calculations were necessary to define the effective geometry (see Fig. 4) as well as lower and upper bound frictions of pendulum systems. For more detailed information, readers are referred to [21].

Table 2. Material and section properties of friction pendulum system

Properties	Type 1	Type 2	Type 3
R1eff = *R4eff* (mm)	2133	3395	6934
R2eff= *R3eff* (mm)	330	526	1074
*d*1*=*d*4* (mm)	339.8	540.4	1103.48
*d*2*=*d*3* (mm)	41.5	65.9	30.85
μ1= μ4 (lower bound)	0.071	0.078	0.093
μ2= μ3 (lower bound)	0.053	0066	0.093
μ (lower bound)	0.068	0.076	0.093
μ1= μ4 (upper bound)	0.085	0.094	0.112
μ1= μ4 (lower bound)	0.064	0.079	0.111
μ (upper bound)	0.082	0.092	0.112

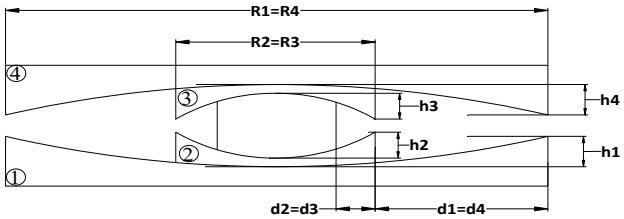

Fig. 4. Geometrical properties of typical friction pendulum system [21].

Effective stiffness was analysed based on iteration approach, similar to lead rubber bearing. Equations (14) to (22) were originally specified in ASCE/SEI 7-10 and was explained in [20]. The analysis was terminated when the ratio of assumed displacement to calculated displacement equals to unity. The significance of the above equations is listed in the Notation section.

$$Q_d = \mu \times \sum W \quad (14)$$

$$Kd = \sum FD/D_D \quad (15)$$

$$\sum FD = W \times n_{bearing} \quad (16)$$

$$Keff = Kd + \frac{Qd}{D_D} \quad (17)$$

$$T_{eff} = 2\pi\sqrt{\frac{\Sigma W}{(K_{eff})(g)}} \quad (18)$$

$$\beta_D = \frac{E}{2\pi K_{eff} {D_D}^2} = \frac{4\mu\Sigma W(D_D - D_y)}{2\pi K_{eff} {D_D}^2} \quad (19)$$

$$D_y = (\mu_1 - \mu_2)R_{eff} \quad (20)$$

$$\beta = \left(\frac{\beta_{eff}}{0.05}\right)^{0.3} \quad (21)$$

$$D'_D = \frac{S_{D1}.{T_{eff}}^2}{4\pi^2\beta} g \quad (22)$$

3 Results and discussion

3.1 Performance level

The performance level of structure featured with seismic isolator LRB and FPS is obtained from the intersecting point between base shear−lateral drift and spectral demand, an example of the result is seen in Fig. 5(a), with detailed responses from all types of bearings, overlaid to each other in Fig. 5(b). In terms of performance level point, structure with and without bearings are still within the range of intermediate occupancy−life safety (IO−SF). However, it is interesting to note that the influence of bearings provides the more ductile response as can be seen from the longer ductile plateau.

Table 4. Base shear and displacement of LRB

Pushover analysis			Time history analysis	
LRB	**Drift (m)**	**Base Shear (ton)**	**Drift *x* (m)**	**Drift y (m)**
1	0.183	89.551	0.162	0.050
2	0.180	89.189	0.149	0.044
3	0.178	89.086	0.145	0.042

Table 5. Base shear and displacement of FPS

Pushover analysis			Time history analysis	
FPS	**Drift (m)**	**Base Shear (ton)**	**Drift *x* (m)**	**Drift *y* (m)**
1	0.116	70.457	0.137	0.045
2	0.102	70.345	0.136	0.053
3	0.082	70.031	0.134	0.043

Furthermore, from the nonlinear structural analysis as summarised in Table 3 and Table 4, it is apparent that FPS-like bearing provides better performance where it is found that the base shear is 28% lower than the LRB-like bearing, suggesting the system denotes higher isolation and thus reducing the seismic forces at the column base. However, the responses for overall bearings demonstrate significant improvement when compared to rigid link structure (see Fig. 5(b) for comparative purposes).

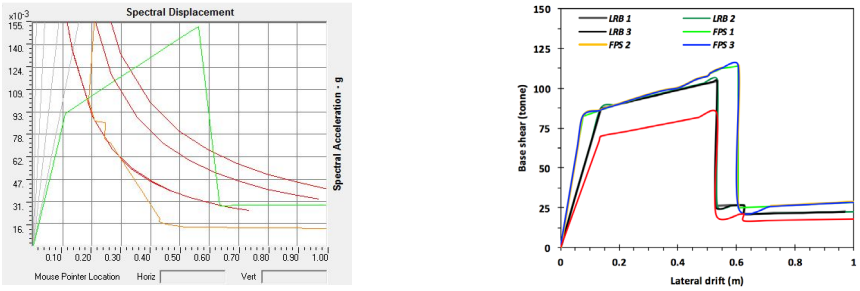

(a) (b)

Fig. 5. Static pushover result. (*a*) performance point and (*b*) overall base shear versus lateral drift

3.2 Plastic hinge mechanism

To gain insight into the formation of plastic hinge over the critical elements LRT structures and to ensure whether or not the onset of plastic hinge transpired firstly at column base, plastic hinge mechanisms are discussed herein. Figure 6 shows step-by-step plastic hinge

formations of the column and bored piles. It is noticeable that the onset development of plastic hinge occurs at the base of the column and propagates toward the foundations, suggesting that foundations are much stronger than the column. It also satisfies to the general conception from seismic provisions that the response modification factor (*R*) of the column is modifiable according to seismic design category while in the foundation, *R* should be unity.

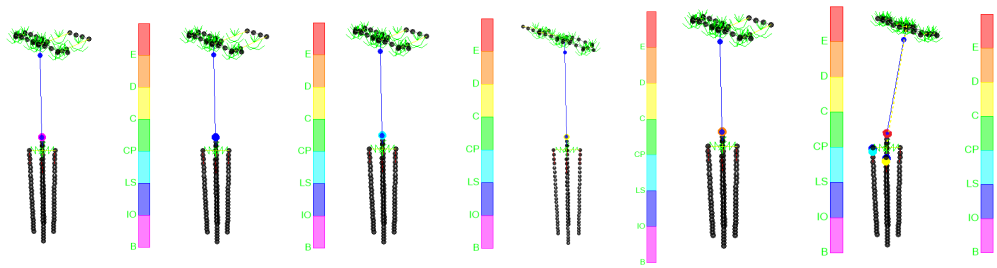

Step 1 (Drift 57mm) **Step 2** (Drift 183mm) **Step 3** (Drift 424mm) **Step 4** (Drift 444mm) **Step 5** (Drift 446mm) **Final step** (Drift 1m)

Fig. 6. Plastic hinge mechanisms of LRT structure

3.3 Energy dissipation

Energy dissipation of the structural members is regarded as one of the fundamental structural capacities that determine their earthquake resistance [22-24]. In this current work, the improvement of energy dissipation controlled by seismic isolation system is inspected by the ratio of the structure without isolator (RL) and with isolators (FPS and LRB). According to Table 5, it is apparent that both seismic isolation devices stipulate higher energy dissipation with average improvement over 15%. Additionally, it is interesting to note that, if compared, energy dissipation of FPS is somewhat greater than LRB, signifying that pendulum systems are rather pleasing.

Table 5. Ratio of energy dissipation

Type	Ratio FPS/RL	Ratio of LRB/RL
1	1.084	1.177
2	1.141	1.180
3	1.165	1.181

3.4 Bearing response

The relationship between time against displacement at bearing for all types of FPS and LRB devices along with rigid link (elastomer) structure is plotted in Fig. 7. The result obtained indicates that structure with elastomer engenders frequent peak facet without significant displacement reduction over time. Whilst in structures with seismic isolation devices, peak facet is found to be relatively diverse with the displacement reduced over time, signifying that seismic isolators provide adequate damping on isolating seismic forces prior to transferring to the column and thereby leading to alleviation of base shear at the column.

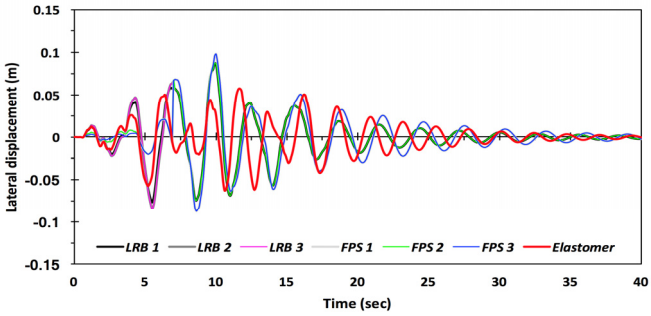

Fig. 7. Time versus lateral displacement non- and seismic isolation devices

4 Conclusions

A comparative study in light rail transit structures featured with lead rubber bearing and friction pendulum system is presented. Nonlinear static and dynamic analysis have been performed to assess the performance of both seismic isolation systems. Based on the structural analysis presented, the following conclusions can be drawn:

1. The application of seismic bearings is found to be helpful in safeguarding the level of performance point of the structure within the range of IO-LS.
2. It is now understood that the use of pendulum bearings indeed provides more ductile response than that of lead rubber bearing. It can also be associated with higher energy dissipation maintained by pendulum bearings.
3. Design of LRT structure has proven to meet the general conception of an earthquake-resistant structure where the development of plastic hinge occurs initially at the column and propagate toward the first two metres of bored pile foundations.
4. It is found that pendulum bearings provides as better response in terms of isolating the seismic force, leading to a decrease of magnitude of base shear at the column base adjacent to the pile cap.

The authors wish to acknowledge the support from PT. ITS Kemitraan for providing relevant data of the LRT project. Gratitude is also expressed to Dr Faimun for his assistance during the completion of this paper.

References

1. B. Budiono, and C. Adella, *Penggunaan isolasi dasar single friction pendulum dan triple friction pendulum pada bangunan beton bertulang*, Jurnal Teknik Sipil, **Vol. 22** No. **2**, pp. 67-78 (2015)
2. S Camelia., Vasile., and Lazar., *Mathematical formulation of friction pendulum system with multiple sliding interfaces*, RJAV, **Vol. 8, No. 1**, pp. 41 (2011)
3. L. Petti, F. Polichetti, A. Lodato, and B. Palazzo, *Modelling and analysis of base isolated structures with friction pendulum system considering near fault events*, Open Journal of Civil Engineering, **Vol. 3**, pp. 86-93 (2013)
4. A. Barmo, I.H Mualla, and H.T. Hasan, *The behaviour of multi-story buildings seismically isolated system hybrid isolation (friction, rubber and with the addition of rotational friction dampers)*, Open Journal Civil Engineering **Vol. 4**, pp. 1-13 (2013)

5. M. Sarkisian, P. Lee, E. Long, D. Shook, and A. Diaz, *Experiences with friction pendulumtm seismic isolation in California*, Earthquake Resistant Engineering Structures, **Vol. 132**, pp. 357-368 (2013)
6. N. Kravchuk, R,Colquhoun, and A. Probaha, *Development of a friction pendulum bearing base isolation system for earthquake engineering education*, Proceedings of the 2008 American Society for Engineering Education Pacific Southwest Annual Conference (2008)
7. R.L. Mayes, *the seismic design handbook*, published in Berkeley, California (2000)
8. T.C. Becker, *Advanced modelling of the performance of structures supported on triple friction pendulum bearing*, Dissertation, Civil and Environmental Engineering, University of California, Berkeley (2011)
9. M. Naguib, F.A. Salem, and K. El-Bayoumi, *Dynamic analysis of high rise seismically isolated buildings*, American Journal of Civil Engineering, **Vol. 3, No. 2**, pp. 43-50 (2015)
10. N.R. Marrs, *Seismic performance comparison of a fixed-base versus a base isolated office building*, Master Thesis, Architectural Engineering, Faculty of California Polytechnic State University, San Luis Obispo (2013)
11. Y.M Al-Anany, and M.J Tait, *Experimental assessment of utilizing fibre reinforced elastomeric isolators as bearings for bridge applications*, Composites Part B, **Vol. 114**, pp. 373-385 (2017)
12. Oiles Corporation, http://www.oiles.co.jp (accessed 16 June 2017)
13. SYSTRA Consulting Group Company, www.systra.com (accessed 1 January 2017)
14. SNI Committee, *Tata cara perencanaan ketahanan gempa untuk struktur bangunan gedung dan non gedung* (SNI-1726-2012), Badan Standarisasi Nasional Indonesia, Jakarta (2012)
15. ASCE Committee, *Minimum Design Loads for Buildings and Other Structures (ASCE/SEI 7-10)*, Structural Engineering Institute, American Society of Civil Engineering, Reston, Virginia (2010)
16. Pusat Penelitian dan Pengembangan Jalan dan Jembatan, Ministry of Public Works and Housing of the Republic of Indonesia, www.pusjatan.com (accessed 3 January 2017)
17. D. Gasparini and E.H. Vanmarcke, *SIMQKE: A Program for Artificial Motion Generation, Department of Civil Engineering*, Massachusetts Institute of Technology, Cambridge, Mass, USA, 1976.
18. AASHTO Committee, *American Association of State Highway and Transportation Officials, Guide Specification for Seismic Isolation Design*, Washington DC (2010)
19. NCHRP 20-7, *Seismic isolation design examples of highway bridges*, Final Report, University of Nevada Reno (2011)
20. Soletanche Freyssinet Group, http://www.freyssinet.com (accessed 7 April 2017)
21. K. EL-Bayoumi, Modelling of triple friction pendulum bearing in SAP2000, International Journal of Advances in Engineering & Technology **Vol. 8 Issue 1** pp. 1964-1971 (2015)
22. A. Tambusay. *Cyclic behaviour slab-column connections using the engineered cementitious composite*, Dissertation, Faculty of Civil Engineering and Planning, Institut Teknologi Sepuluh Nopember, Surabaya, Indonesia (2017)
23. A. Tambusay., P.Suprobo., Faimun, and A.A Amiruddin., *Finite element modelling of a reinforced concrete slab-column connection under cyclic lateral load*,

International Journal of Applied Engineering Research, ISSN 0973-4562, **Vol. 12**, **No. 9**, pp. 1987-1993 (2017).

24. A. Tambusay., P.Suprobo., Faimun, and A.A Amiruddin., *Finite element analysis on the behaviour of slab-column connections using PVA-ECC material*, Jurnal Teknologi (Science and Engineering), **Vol. 79, No. 5**, pp. 23-32 (2017)

Notations

Q_{dj}	Characteristic strength of the isolator unit at support "i"	μ_1	friction for surface 1 and 4
Q_{di}	Characteristic strength of the isolator unit at support "j"	μ_2	friction for surface 2 and 3
Q_d	Characteristic strength of the isolator unit	W	Vertical Load
K_{dj}	Post elastic stiffness at support "j"	β	Damping reduction factor
K_{di}	Post elastic stiffness at support "i"	n	number of isolation seismic
$K_{sub,i}$	Stiffness of substructure at support "i"	K_{sub}	Stiffness of substructure
$K_{sub,j}$	Stiffness of substructure at support "j"	α_j	Effective stiffness
k	Effective stiffness of the isolator	ξ	Equivalent viscous damping ratio
d	total deck displacement relative to ground (*assumption*)	β_{eff}	Effective damping reduction factor
$d_{isol,j}$	Isolation displacement at support "j"	d_{isol}	Isolation displacement
$d_{sub,j}$	Substructure displacement at support "j"	d_{sub}	Substructure displacement
g	Gravitational acceleration (9.81 m/sec^2)	$F_{sub,j}$	Substructure force at support "j:
T_{eff}	Period seismically isolated structure in the direction under consideration		
K_{eff}	The sum of effective linear stiffnesses of all bearing		
B_L	Damping coefficient for the long period range of the design response spectrum.		
S_{D1}	Horizontal response spectral acceleration coefficient at 1.0 s period modified by long- period site factor		
K_d	The second slope stiffness of the bilinear hysteresis curve		
μ	Force at zero displacement divided by the normal load		
D_D	Displacement assumption for upper bound analysis		